

### 3. Computational Investigation of Epithelial Cell Dynamic Phenotype In Vitro\*

#### 3.1. Background

In 3D cultures, epithelial cells such as Madin-Darby canine kidney (MDCK) cells engage an array of mechanisms and activities to develop stereotypical cystic organoids (O'Brien et al., 2002; Martín-Belmonte et al., 2008). What strategy will enable linking knowledge of molecular mechanisms and cell level events and activities to features of cystogenesis for a deeper understanding of the phenomena? What cell actions characterize different stages of cystogenesis? How are those actions contributing to cystogenesis? The emergence of stable organoid structures is the cumulative consequence of individual cell actions: the system's dynamic phenotype. Disruption of one or more of these actions can cause potentially pathologic changes (Debnath and Brugge, 2005). A strategy to answer the preceding questions must include classifying essential cell actions and tracing their relative use and roles during cystogenesis. Using time-lapse, microscopy images alone it can be difficult to ascertain what cell actions are responsible for the observed structure transformations.

The computational methods detailed herein provide an alternative approach to gaining the much needed insight. I used in silico epithelial analogues (ISEAs) that have undergone validation against a targeted set of Madin-Darby canine kidney (MDCK) epithelial cell attributes. I revised the earlier analogue (ISEA1), developed by Grant et al. (2006), in stages to achieve increased phenotype overlap between the revised analogue (ISEA2) and MDCK cell cultures. To keep improvements parsimonious, I expanded the list of targeted attributes by one: all stable cyst structures must have a convex contour. No irregular margins or dimples were allowed. ISEA1 failed to validate against that attribute. Through exploratory simulations, I discovered and added one new cell action to achieve the additional attribute. The mappings from in silico components, their spatial arrangement, their mechanisms of interactions, and system-level attributes to their in vitro counterparts (Fig. 1.2) improved following that refinement.

Cell biologists compare and contrast the growth characteristics of different, related epithelial cell lines in part to better understand how and where their behaviors differ or are similar. That knowledge can be used to make better inferences about referent cell behaviors *in vivo*. A proven

---

\* This chapter has been submitted to *Theoretical Biology and Medical Modelling*

wet-lab approach is to design and conduct experiments to test hypotheses about cell line responses to interventions, such as blocking a signaling pathway or a cell surface receptor. Analogous methods must be used to study and compare phenotypic attributes of *in silico* analogues, such as ISEA1 and ISEA2. In addition, study of analogue responses to interventions improve insight into MDCK morphogenesis. Differences in morphological and dynamic phenotype, or lack thereof, between two analogues could shed additional insight on those of the referent (Park et al., 2009). With that in mind, I compared ISEA1 and ISEA2 behaviors to understand how specific mechanistic changes alter their morphogenic attributes.

Each simulation cycle, each ISEA cell assessed the current arrangement of neighbors and then selected an action, which it always executed. The resulting process achieved validation. Are actions of MDCK cells in cultures (and epithelial cells in general) so rigidly choreographed? How tightly must ISEA adhere to its operating principles before aspects of phenotype become measurably abnormal? I gained insight into plausible answers by systematically relaxing two, key ISEA actions and exploring in detail the phenotypic consequences. One action mapped to anoikis, a specific category of cell death. The other involved directed placement of an ISEA daughter cell, a form of oriented cell division. The ISEA1 phenotype was quite sensitive to dysregulating the two actions: engaging in either action less than 80% of the time caused easily detected phenotypic changes. Interestingly, ISEA2 was more robust to identical disruptions. Both ISEA1 and ISEA2 exhibited phenotypes that resembled those associated with an *in vitro* model of early glandular epithelial cancer (discussed in Chapter 4). To the extent that the *in silico*-to-*in vitro* mappings in Fig. 1.2 are valid, ISEA2's operating principles and dynamic phenotype stand as hypotheses of their MDCK counterparts in cell culture.

## 3.2. Methods

### 3.2.1. Modeling approach

Traditional inductive modeling and the approach used herein present different yet complementary approaches to exploring explanations of biological phenomena. Models of the former type are usually built by first analyzing data, creating a mapping between the envisioned system structure and components of the data, and then representing the generation of those data components with mathematical equations. Inductive analytical models test hypotheses about data. The method relies heavily on the researcher's knowledge combined with induction. When successful, it creates models that can extrapolate beyond the original data, making the method

ideal for prediction. The class of models and methods described herein are different (Hunt et al., 2008). They are designed primarily to develop, test, and refine mechanistic explanations or hypotheses about biological phenomena. They are what Fisher and Henzinger (2007) have referred to as executable biology. For a specific referent system, one first identifies the perspective taken in the wet-lab along with the system aspects on which to focus, and then states the uses to which the model would be put. Next, building blocks and their functions, along with assembly methods are proposed so that the components and assembled system map logically to wet-lab counterparts, as illustrated in Fig. 1.2. The *in silico* system is referred as an analogue to help distinguish this class of models from traditional, inductive models. Analogues are executed and measured in the same way as their referents. Data accumulated during executions are compared against data taken from the referent. When an analogue fails validation, it must be revised, and validated against its predecessor (cross-model validation) and then against referent attributes. When satisfaction is achieved, a case can be made for each of the mappings in Fig. 1.2. The assembled components and their operating methods stand as a hypothesis: these mechanisms will produce targeted characteristics. Execution tests that hypothesis. The methods provide for establishment of plausible reductive hierarchies between lower level mechanisms and higher-level phenomena by growing useful, more detailed *in silico* analogues from a predecessor.

### **3.2.2. Model design requirements**

To achieve both short and long term goals, I needed models and components that met the following five basic requirements. 1) Model components must be modular. Components, analogous to referent counterparts, are designed to interact. It must be easy to join, disconnect, or replace components without altering the functions and interrelations of other components. 2) The composed system must be flexible. It must be relatively simple to change usage and assumptions, or increase or decrease analogue detail in order to meet the particular needs of a new experiment, without requiring significant system reengineering. 3) System components must be reusable and adaptable for simulating epithelial cell behaviors in different experimental conditions in the presence and absence of treatments and interventions. 4) Analogues need to be articulated, multi-component systems that can be expanded easily to represent additional details or mimic additional referent attributes. 5) Components and methods need to be designed so that they can be replaced easily with alternate or more detailed counterparts, when needed.

### **3.2.3. Discrete event simulations using agents**

To achieve the above requirements, I adapted agent-based modeling (Grimm et al., 2005) and discrete event simulation (Law and Kelton, 2000; Zeigler et al., 2000) methods. In agent-based modeling, a system is comprised of quasi-autonomous, decision-making entities called agents. An agent follows a set of rules that governs its actions and interactions with other system components. Agent-based modeling facilitates creating systemic behaviors and attributes that arise from the purposeful interactions of components. The resulting models have advantages when attempting to understand and simulate phenomena produced by systems of interacting components. I used quasi-autonomous agents to represent epithelial cells. I also employed quasi-autonomous components outside of the simulated biology for experimentation and analysis (Fig. 3.1), but still within the computational framework. In discrete event simulations, system operation is represented as a temporal sequence of events, occurring within discrete time intervals. System state evolves during those discrete time intervals. Using such methods facilitated encapsulating system operations and conceptualizing complex dynamics. The methods provided a rigorous formalism for managing modularity and hierarchy in space and time. From a simulation perspective, activities such as cell division, death, and polarization could be represented as being discrete. Stochasticity, which is natural to both agent-based modeling and discrete event simulations, was introduced mostly in the form of probabilistic parameters that regulated agent actions and execution order.

### **3.2.4. In silico experimentation framework**

ISEA1 and ISEA2 comprise the core analogue and system-level components for experimentation and analysis (Fig. 3.1). Because ISEA2 is based on ISEA1, both share a common design, and their experiment features overlap significantly (discussed below). Before moving forward with model refinement and experimentation, implementation redundancies of ISEA1 and ISEA2 were removed. I revised the existing framework to enable simulation of multiple, somewhat different CELL analogue types. ISEA1 was ported and revalidated within the new framework prior to ISEA2 development. To clearly distinguish ISEA components and processes from their in vitro counterparts, hereafter I use small caps when referring to the former.

I created system-level components including EXPERIMENT MANAGER, OBSERVER, and CULTURE graphical user interface (GUI) to enable semi-automated experimentation and analysis. EXPERIMENT MANAGER, the top-level system component, is an agent that provides experiment protocol functions and specifications. The specifications define the mode of experimentation and the system's parameter vector. Experiments can be conducted in default, visual, or batch modes.

Batch mode enables automatic construction and execution of multiple experiments, as well as processing and analysis of recorded measurements. Based on user-defined specifications, EXPERIMENT MANAGER automatically generates a set of parameter files and executes a batch of experiments, each corresponding to a different parameter file. After completion of all experiments, basic analytic operations collect and summarize data. OBSERVER is responsible primarily for recording measurements. At the end of every simulation cycle, OBSERVER scans the CULTURE internals and performs measurements. The measurements are recorded as time series vectors. At simulation's end, data are written to a set of files for analytic processing by EXPERIMENT MANAGER. CULTURE GUI provides a visualization console, which can be used interactively to start or pause a simulation and to access live states of CULTURE grid content. Using CULTURE GUI functionalities, OBSERVER can capture time-lapse CULTURE images and store them in multiple formats for post-processing.

### **3.2.5. In silico culture components**

Detailed descriptions of ISEA1 design features, and development methods, are available in (Grant et al. 2006). ISEA2 design uses similar features, which have been refined to meet study requirements. An abridged description follows. The referent in vitro cell culture was conceptually abstracted into four components: cells, media containing matrix (matrix hereafter), matrix-free media (free space hereafter), and a space to contain them. Discrete software objects with eponymous names represent the essential cell culture components: CELL, MATRIX, FREE SPACE, and CULTURE. MATRIX and FREE SPACE are passive objects. A MATRIX object maps to a cell-sized volume of ECM. A FREE SPACE object maps to a similarly sized volume of material that is essentially free of cells and matrix elements. FREE SPACE also represents luminal space and non-matrix material in pockets enclosed by cells. The latter are called LUMINAL SPACE when distinction from FREE SPACE is useful. CELLS are quasi-autonomous agents (as agents, they can schedule their own events; they follow their own agenda). They use a set of rules or decision logic to interact with their local environment. A CULTURE is an agent that maps abstractly to a cell culture within one well of a multi-well culture plate. The CULTURE uses a standard two-dimensional (2D) hexagonal grid to provide the space in which its objects reside. The grid has toroidal topologies. For simplicity, each grid position is occupied by one object. That condition can be changed when the need arises.

### 3.2.6. ISEA execution protocol

A CULTURE has base methods that are called automatically at a simulation's start and end. The start function initializes the grid and CULTURE components, CELLS, MATRIX, and FREE SPACE. Simulation starts upon completion of that process. As execution advances, the event schedule is stepped for a number of simulation cycles or until a stop signal is produced. At simulation's end, the CULTURE finish function closes open files and clears the system.

Simulation time is advanced discretely, and is maintained by a master event schedule. Event ordering within a simulation cycle is pseudo-random. Having objects update pseudo-randomly simulates the parallel operation of cells in culture and the nondeterminism fundamental to living systems, while building in a controllable degree of uncertainty. Within a simulation cycle, each CELL in pseudo-random order is given an opportunity to interact with adjacent objects in its environment and, if required, undertake an action. Every CELL uses the same step function. A set of CELL axioms (Fig. 3.2) determines all CELL actions. A CELL selects just one axiom and corresponding action during each simulation cycle.

### 3.2.7. Axiomatic operating principles

An agent has rules and protocols for interacting with external components. Rules can take any form. I elected to have all rules take the form of axioms. I use the term “axiom” to reinforce an idea that the computational model is a mathematical, formal system and that analogue execution is a form of deduction from the original axioms or assumptions explicitly programmed into the model. An axiom specifies a precondition and corresponding action. I specified what I judged to be a minimal set of action options: replace an adjacent non-CELL object with a CELL copy, DIE (vanish) and leave behind a LUMINAL SPACE, create MATRIX, destroy an adjacent non-CELL object and move to that location leaving behind a LUMINAL SPACE, POLARIZE, DEPOLARIZE, and do nothing. For any precondition, only one action option was executed.

ISEA1 had eleven axiomatic operating principles that enabled the analogue to validate against its initial targeted attributes. For convenience, the final ISEA1 axioms are summarized as follows. The precondition applies to the six objects adjacent to each CELL.

1. All neighbors are CELLS: DIE (delete self) and leave behind a LUMINAL SPACE.
2. All neighbors are LUMINAL SPACE: DIE and leave behind a LUMINAL SPACE.
3. All neighbors are MATRIX: replace a randomly selected MATRIX with a CELL copy.

4. Neighbors comprise one CELL and LUMINAL SPACES: add MATRIX between self and the adjoining CELL.
5. Neighbors comprise at least two CELLS and LUMINAL SPACES, but no MATRIX: DIE (undergo ANOIKIS) and leave behind a LUMINAL SPACE.
6. Neighbors comprise at least one CELL and MATRIX: create a CELL copy; the copy replaces any MATRIX that maximizes its number of CELL neighbors.
7. Neighbors comprise at least two LUMINAL SPACES and MATRIX: create a CELL copy; the copy replaces any LUMINAL SPACE that adjoins MATRIX.
8. Neighbors comprise CELLS, MATRIX, and at least two adjacent LUMINAL SPACES: create a CELL copy; the copy replaces any LUMINAL SPACE neighbor that adjoins MATRIX and LUMINAL SPACE.
9. Two CELL neighbors are separated on one side by MATRIX and on the other side by LUMINAL SPACE: POLARIZE.
10. A POLARIZED CELL has noncontiguous MATRIX neighbors: revert to NONPOLARIZED CELL state.
11. None of the preceding preconditions has been met: do nothing; CELL mandates achieved.

Starting with the ISEA1 axioms, I devised, tested, and iteratively refined candidate axioms to enable the CELLS to consistently develop CYSTS with smooth margins and a convex shape (in the hexagonal grid representation), while validating for the targeted attributes described in (Grant et al., 2006). At each step, variations of an axiom were tested, and those that moved the analogue closer to validation were selected for further refinement. In its validated form, ISEA2 used Axioms 1–10 from ISEA1 without change. However, ISEA1’s Axiom 11 was replaced by the following two axioms.

11. Neither the preceding nor the following preconditions have been met: do nothing; CELL mandates achieved.
12. A POLARIZED CELL confirms that Axiom 9 precondition is met and has only one MATRIX neighbor: the POLARIZED CELL deletes the adjacent MATRIX, moves to its location, and leaves behind a LUMINAL SPACE.

The revised axioms diagrammed in Fig. 3.2 represent what I determined as a minimal change that was required for final validation. Revisions that were more elaborate also enabled those ISEAs to achieve the target attributes. However, they were rejected because they were not parsimonious. The final validation required that > 98% of the CYSTS formed during 50

simulation cycles in 100 Monte Carlo simulations must have a roundish, convex shape (visually inspected).

### 3.2.8. Operational disruption of ISEA CELL axioms

I implemented a method to disrupt selectively the operation of individual CELL axioms. I added a parameter,  $p$ , for each axiom. It controlled the probability of the decision-making CELL electing to follow the axiom when its precondition applied. Parameter values ranged from 0 to 1 inclusively. A parameter value = 1 corresponded to 100% adherence. Setting it to zero completely blocked the prescribed action and, as specified, dictated an alternate action. An additional control was added to allow the CELL to draw a pseudo-random number (PRN) from the standard uniform distribution at each decision point. The axiom's prescribed action was followed only when the PRN was  $\leq$  the probability threshold set by its parameter.

I considered, and used when applicable, alternative actions that map to plausible in vitro cell actions occurring in a dysregulated state. Axioms 1, 2, and 5 governed CELL DEATH; a reasonable alternative was to remain ALIVE (i.e., do nothing). Axiom 3 dictated non-directional CELL DIVISION; its alternate action was to do nothing (i.e., prevent REPLICATION). I also assigned the alternate action of 'do nothing' to Axiom 4 (MATRIX production). Several dysregulated action options were available for Axiom 6 (directed CELL DIVISION). One was to do nothing, effectively suppressing CELL DIVISION. Another was DISORIENTED CELL DIVISION, positing the CELL copy in a random direction without regard for the number of CELL neighbors. I elected to use the latter, for which adequate, supportive biological information is available. Axiom 7, which dictated CELL DIVISION, had available the same alternative action options. Axiom 8 (CELL DIVISION or POLARIZATION) had a precondition comprising all three component types (CELL, MATRIX, and LUMINAL SPACE), which presented many plausible action options. One option was preventing CELL DIVISION; another was to allow the CELL to DIVIDE non-directionally as described above. Another option was to initiate POLARIZATION. The remaining axioms, Axioms 9-12, posed a similar problem of having many plausible action options. Because no wet-lab experimental insight was available to narrow the options, I elected to defer investigation of those axioms until more information becomes available.

### 3.2.9. Simulation experiment design

The following describes design and execution of ISEA1 and ISEA2 simulation experiments. First, the top-level system component, EXPERIMENT MANAGER, was initialized. Next,

EXPERIMENT MANAGER created a new CULTURE and filled its grid with MATRIX. The grid width and height were set to 100. CULTURE initialized a PRN generator with a seed set to the system's clock. A new seed was used to initialize the CULTURE'S PRN generator at the start of each simulation. Pseudo-random seeds were generated from the CULTURE'S PRN generator to initialize those used by CELLS. Following CULTURE grid setup, one CELL was placed at the center of the CULTURE grid, replacing an existing MATRIX object. The simulation started when the initialization of the CULTURE contents was completed. Each simulation experiment comprised 100 Monte Carlo (MC) runs. Each MC run was executed for 50 simulation cycles. After simulation, the recorded measurements were written to files and the CULTURE was destroyed. A new CULTURE was created for each repetition.

### 3.2.10. Implementation tools

The model framework was implemented using MASON Version 11. MASON (<http://cs.gmu.edu/~eclab/projects/mason>) is a discrete-event, multi-agent simulation library coded in Java. The analogues were developed in an integrated application development platform, NetBeans 5.5 (<http://www.netbeans.org>). Batch simulation experiments were performed on a small-scale Beowulf cluster system. Computer codes and project files are available in Supplemental DVD.

## 3.3. Results

To validate against the targeted attributes, a single CELL was placed in CULTURE space, surrounded by MATRIX. As simulation progressed, the CELL underwent repeated rounds of replication, followed by LUMINAL SPACE formation and CYST maturation. The LUMINAL SPACE grew as CELLS in the inner region DIED (and vanished). Growth characteristics were similar to those observed in MDCK embedded cultures (Fig. 3.3A). CULTURES always formed stable CYSTS bordered by POLARIZED CELLS (Fig. 3.3B, C). Most ISEA1 CYSTS had irregular shapes. ISEA2 consistently produced CYSTS having a roundish, convex shape (Fig. 3.3C). CYSTS in ISEA2 CULTURES stabilized with fewer CELLS (Fig. 3.3D).

At the start of an EMBEDDED CULTURE simulation, a single CELL was placed in CULTURE space, surrounded by only MATRIX. As a simulation progressed, the CELL underwent repeated rounds of CELL REPLICATION, followed by the formation of LUMINAL SPACE and an increase in CELL number and CYST diameter. The central LUMINAL SPACE grew as CELLS in the inner region

DIED or moved out. The growth dynamics and final phenotype were similar to those observed for MDCK cells. The EMBEDDED CULTURE always formed stable CYSTS bordered by POLARIZED CELLS, and ISEA consistently produced CYSTS with a roundish, convex shape with smooth margins. During an occasional simulation, because of their changing, local environment one or more CYST surface CELLS failed to POLARIZE or DIE before the simulation ended. Such events prevented the local rounding out process that a POLARIZED CELL can undertake, preventing a few structures from stabilizing within 50 simulation cycles.

For dysregulation experiments, I focused on two critical CELL axioms, Axioms 5 and 6. Axioms 2, 3, 4, and 7, were not critical to CYST formation in EMBEDDED CULTURE (they were critical in other CULTURE conditions, such as monolayer), and were infrequently used, so they were excluded from detailed analysis. Although not essential for EMBEDDED CULTURE, Axiom 4 proved to be an important yet rare event axiom, as discussed below. Disrupting Axiom 8 is not straightforward: if the axiom is not applied, some alternative action must follow from its precondition, and there are many plausible options. I elected not to pursue disruption of Axiom 8 until further insight from wet-lab studies becomes available to narrow options. Disrupting Axiom 1 was straightforward, but the results (not shown) offered no significant insight: CLUSTERS either developed normally into CYSTS for  $p > 0$  or grew unchecked as a solid mass when  $p = 0$ . I expected that outcome because Axiom 1 was required for initial LUMINAL SPACE creation but became nonessential thereafter. On the other hand, Axioms 5 and 6 were essential to CYST formation. Anoikis is a form of cell death that epithelial cells undergo when they lose direct matrix contact (Boudreau et al., 1995). Axiom 5 dictates ANOIKIS. It is the most frequently used CELL DEATH axiom in both ISEA1 and ISEA2. Axiom 6 dictates directed CELL creation (the event maps to selective placement of a daughter cell), and accounts for most of the CELL creation events in both analogues. The in vitro counterparts of Axioms 5 and 6 are centrally implicated in epithelial morphogenesis and carcinogenesis, and have been shown to be important in the context of in vitro cell cultures.

### 3.3.1. Dysregulation of Axiom 5 (ANOIKIS)

In MDCK cultures, blocking apoptosis has been shown to cause cyst lumen filling (Debnath et al., 2002). I speculated that if ISEA CELL actions have MDCK counterparts, then the two analogues should exhibit (predict) LUMEN filling when ANOIKIS is compromised. I simulated the condition by disrupting application of Axiom 5. So doing caused aberrant growth (Fig. 3.4) and

changed CELL activity patterns (Fig. 3.5). Growth rates increased nonlinearly with increasing dysregulation. ISEA1 was more sensitive to dysregulation at mid-range  $p$  of 0.4 and 0.6 than was ISEA2. No marked differences were noted at other tested levels. CELL population measurements after 50 simulation cycles reflected changes in growth (Fig. 3.4C). ISEA2 (vs ISEA1) produced structures having fewer CELLS.

The CULTURE morphology became irregular with increased dysregulation (Fig. 3.6). Relative to ISEA2, irregularities were more pronounced when ISEA1's Axiom 5 was dysregulated. When CELL creation events outpaced DEATH, small, inverted CYSTS formed and stabilized (through POLARIZATION) within LUMENS. As dysregulation increased, surface irregularities postponed POLARIZATION enabling further CELL creation events and surface expansion. For ISEA2, other factors contributed to LUMEN clearing. The convexity drive (Axiom 12) enabled surface CELLS to POLARIZE sooner. It also retarded inverted CYST formation by CELLS trapped within LUMENS. Trapped CELLS were thus more likely to satisfy the precondition of Axiom 5, even when Axiom 5 was partially dysregulated. See Chapter 4 for further analysis of ISEA2 dysregulation.

Figure 3.5 shows how changes in CELL activity patterns accompanied morphology changes for two levels of Axiom 5 dysregulation. ANOIKIS dysregulation changed the occurrence frequencies of axiom preconditions. That change resulted in increased CELL creation events for both ISEA1 and ISEA2. Interestingly, for  $p = 0.8$  and 0.6, those changes led to a net increase in CELL DEATH events. For ISEA1, many of the additional CELL creation events occurred along the CYST's outer edge, whereas for ISEA2, many of the additional CELL creation and DEATH events occurred within the LUMEN. The CELL creation events within LUMENS were enabled by the Axiom 4 action: create MATRIX between two CELLS. Blocking Axiom 4 use blocks most all CELL creation events within LUMENS and promotes LUMEN clearance (not shown).

### 3.3.2. Dysregulation of Axiom 6 (oriented CELL creation)

Experimental evidence suggests that cell division has a specific orientation of the division axis (Théry et al., 2005; 2007). Similar to its in vitro counterpart, CELL creation from Axiom 6 was oriented (not random). I dysregulated Axiom 6 by allowing the decision-making CELL to place a new CELL in a randomly selected MATRIX location, rather than selecting one that maximizes CELL contact. The overall results are shown in Fig. 3.7. CULTURE growth rate and CELL count after 50 simulation cycles increased monotonically with Axiom 6 dysregulation. The changes were less dramatic than those observed following Axiom 5 dysregulation, and there were marked differences between dysregulated ISEA1 and ISEA2 CULTURE growth. ISEA2 was less

susceptible to disoriented placement of a newly created CELL. Mean CELL count in ISEA2 CULTURES was always smaller than that for ISEA1 at every tested dysregulation level.

Dysregulating Axiom 6 using  $p = 0.8$  and  $0.6$  increased CELL DEATH and CELL PROLIFERATION activities of ISEA2 less than ISEA1 (Fig. 3.5). CELL DEATH events were offset by an approximately equal number of CELL creation events, and that was consistent with the observation that LUMEN-entrapped CELLS underwent cycles of CELL creation and DEATH. Additional results for ISEA2 dysregulation are provided in Chapter 4.

Inspection of Fig. 3.6C, D shows that the morphological irregularities resulting from a given degree of Axiom 6 dysregulation were less pronounced than from a corresponding degree of Axiom 5 dysregulation. For ISEA1, the morphology change produced by a degree of Axiom 6 dysregulation was very similar to that caused by a lesser degree of Axiom 5 dysregulation. ISEA1 structures produced using dysregulated Axiom 6 contained a larger fraction of POLARIZED CELLS than did corresponding Axiom 5 dysregulated structures, and so the former changed more slowly as simulations progressed. For ISEA2, because all CELL DEATH axioms were always followed, there was less LUMEN filling when Axiom 6 was disrupted, compared to when Axiom 5 was disrupted to the same degree. As noted above, ISEA2 LUMEN filling was enabled by Axiom 4. Blocking it severely restrained and often eliminated formation of INTRALUMINAL CELL CLUSTERS.

### 3.3.3. Dynamic phenotype

Figure 3.8 presents dynamic phenotype: the normalized frequency of axiom use by both ISEA1 and ISEA2. The CYSTOGENESIS mechanism at any stage in the process is the set of all events occurring within that interval. It is clear from Fig. 3.8 that there is no specific CYSTOGENESIS mechanism. From start to the end of a simulation or until a stable structure forms, the mechanism evolves. How it evolves is a feature of that analogue's dynamic phenotype. Use patterns were similar for those axioms common to both analogues and that were used most frequently (1, 3, 5, 6, 9, and 11). Major differences were evident only for the less frequently used axioms (2, 4, 7, 8, and 10). As noted earlier, enabling CELL movement (Axiom 12) had an unanticipated consequence: it enabled the occasional formation of long-lived, small islands of CELLS within a LUMEN. Once a unit of MATRIX was formed, CELLS within a LUMEN could move and that gave rise to preconditions for creation of new CELLS as well as CELL DEATH. The process can continue for an extended interval and that accounts for the very low frequency of use of Axioms 2, 4, 7, and 8 by ISEA2. Note that when CELLS are trapped within an otherwise stable

CYST, those INTRALUMINAL events are the only events. For that simulation, their relative use frequencies are large, and it is those values that are averaged with the values from other simulations, which are typically zero.

If nutrient levels within lumens are less than outside the cyst, then intraluminal cell division may not be sustainable. Furthermore, under 3D culture conditions, there is no direct evidence of matrix production by MDCK cells trapped within early-stage lumens during cystogenesis. It is noteworthy that by simulation cycle 50, when Axiom 4 is blocked, ISEA2's use frequency of axioms 2, 7, 8 and 10 drops to zero (not shown): ISEA2's axiom frequency of use pattern becomes similar to that of ISEA1.

Axiom dysregulation changed dynamic phenotype. Because trends are similar for ISEA1 and ISEA2, I present in Figs. 3.9 and 3.10 selected results for ISEA2. Figure 3.9 shows ISEA2 axiom use frequencies for Axiom 5  $p = 0.8$  and  $0.6$ . The major consequence was reduction in Axiom 11 usage (do nothing: mandates achieved). That decline was mirrored by the rise in Axiom 5\* (dysregulated action) usage, which remained relatively constant after five simulation cycles. In parallel, the use patterns for all other axioms changed relative to their  $p = 1$  patterns. Even though only Axiom 5 was disrupted occasionally, all ISEA2 operating principles were impacted to some extent: the entire dynamic phenotype changed. However, the morphological consequences for  $p = 0.8$  were difficult to detect: except for a tendency to be larger, most stabilized CYSTS were indistinguishable from those formed when  $p = 1$ . The potential morphological consequences of relaxing Axiom 5's  $p$  by 20% were thwarted by small shifts in the use frequencies of all other axioms. This observation suggests that the networked nature of ISEA2 axiom usage acts to buffer the consequences of small disruptions of any one operating principle.

Both the morphological and dynamic phenotypic consequences of Axiom 6 dysregulation were less dramatic than were those of Axiom 5. They were also less dramatic in ISEA2 than in ISEA1. Reducing  $p$  led to larger structures that eventually stabilized (Fig. 3.7B) and to more CELLS being trapped within occasional LUMENS (Fig. 3.6D). Comparison of Figs. 3.9 and 3.10 reveals that the influence of Axiom 6 disruption was also less significant than that of disrupting Axiom 5 to the same degree. For  $p = 0.8$  and  $0.6$ , the activities of CELLS trapped in LUMENS were primarily responsible for increased axiom use after about 20 simulation cycles. When Axiom 4 was blocked (not shown), those axiom use frequencies diminished considerably making an increased CYST size the primary consequence of Axiom 6 disruption.

### 3.4. Discussion

I detailed a computational approach to build and test plausible hypotheses of in vitro dynamic phenotype. The newly developed framework enabled MDCK cell-mimetic analogues to function as autonomously as feasible for software agents. Axiomatic operating principles enabled ISEA2 CELLS to consistently produce convex CYSTS under simulated 3D embedded culture condition. Measures of axiom use during CYSTOGENESIS provided a detailed description of ISEA2 dynamic phenotype. Dysregulating key CELL DEATH and DIVISION axioms led to disorganized cystic forms that were reminiscent of the in vitro tumor reconstruction phenotype. Unexpectedly, ISEA2's drive for convexity made it less susceptible to, or more robust against, the dysregulation of either axiom when compared to its predecessor, ISEA1. It will be interesting to learn if the mechanisms underlying epithelial cyst convexity in cultures contribute to robustness against comparable interventions. In addition, occasional disruption of one activity in a minority of CELLS, as in Figs. 3.9 and 3.10, had consequences for the system (e.g., altered CYST morphology) and for all other normal behaving CELLS. The average axiom use patterns of all other CELLS changed. Upon reflection, the observation could be expected. The actions of all CELLS in a CLUSTER transforming into a CYST are networked in space and time. An action of one CELL can effect the action options of a nearby CELL at a future time. If a CELL occasionally malfunctions, it has measurable consequences, as shown in Figs. 3.9 and 3.10. To the extent that the mappings in Fig. 1.2 are accepted as valid, I can extend such observations to epithelial cells undergoing morphogenesis.

Cell processes work together in ways that give rise to effective mandates that normal epithelial cells appear to follow. Each mandate is assumed a consequence of the interoperation of genetics and environmental factors. How specific cell actions contribute to these mandates is unclear. However, tracing CELL activities during ISEA2 simulations makes clear how their mandates, the targeted attributes, are achieved. That clarity provides insight into and plausible explanations of MDCK's morphogenic phenomena. Because ISEA components and mechanisms are coarse-grained, one ISEA2 axiom may map to many fine-grain MDCK processes. Iterative refinement of ISEA2 so that it achieves an expanded set of MDCK attributes will improve and concretize the mappings from analogue to MDCK cultures, potentially creating new knowledge. Mappings from specifics of MDCK cultures (complex) to analogue (simplified), however, will always be ambiguous, a property of all referent-model pairs.

The nature and organization of software components within the ISEA framework, as illustrated in Fig. 3.1, were designed to facilitate iterative refinement of everything on the right

side of Fig. 1.2. That process can concretize each of the mappings from ISEA to MDCK counterparts. As the process continues, following each round of validation, more of what we know or think we know becomes instantiated in the analogue. After many such rounds, the analogue will begin transforming into an executable knowledge embodiment. To achieve that vision, it is essential that biomimetic components function (quasi-) autonomously, all or part of the time. That is why CELLS are agents. Everything that a CELL needs to function (in a specified software environment) is contained within its code. Absent that property, the mappings from ISEA to MDCK cystogenesis mechanisms are not concretizable, and so the mappings from ISEA to MDCK operating principles are forced to remain conceptual.

In summary, the MDCK analogues described herein provided for a hypothesis—a theory—of how the collective consequences of individual MDCK cell actions might give rise to systemic *in vitro* phenotype. The causal chain of events responsible for most ISEA behaviors could be explored in detail, and assessments could be made of their relative roles during simulation. Having that capability enabled us to develop a detailed dynamic ISEA phenotype. The MDCK embedded culture counterpart is problematic to obtain using state-of-the-art *in vitro* methods. I expect future rounds of model refinement and validation will strengthen *in silico*-to-*in vitro* mappings, thus providing a viable strategy to gain deeper insight into the mechanistic basis of epithelial cystogenesis, morphogenesis, and *in vitro* transformations.

## References

1. Baena-López LA, Baonza A, García-Bellido A (2005) The orientation of cell divisions determines the shape of Drosophila organs. *Curr Biol* 15:1640-1644.
2. Bryant DM, Mostov KE (2008) From cells to organs: building polarized tissue. *Nat Rev Mol Cell Biol* 9:887-901.
3. Debnath J, Mills KR, Collins NL, Reginato MJ, Muthuswamy SK, Brugge JS (2002) The role of apoptosis in creating and maintaining luminal space within normal and oncogene-expressing mammary acini. *Cell* 111:29-40.
4. Debnath J, Brugge JS (2005) Modelling glandular epithelial cancers in three-dimensional cultures. *Nat Rev Cancer* 5:675-688.
5. Galle J, Loeffler M, Drasdo D (2005) Modeling the effect of deregulated proliferation and apoptosis on the growth dynamics of epithelial cell populations *in vitro*. *Biophys J* 88:62-75.
6. Gong Y, Mo C, Fraser SE (2004) Planar cell polarity signalling controls cell division orientation during zebrafish gastrulation. *Nature* 430:689-693.

7. Grant MR, Mostov KE, Tlsty TD, Hunt CA (2006) Simulating properties of in vitro epithelial cell morphogenesis. *PLoS Comput Biol* 2:e129.
8. Martín-Belmonte F, Yu W, Rodríguez-Fraticelli AE, Ewald AJ, Werb Z, Alonso MA, Mostov K (2008) Cell-polarity dynamics controls the mechanism of lumen formation in epithelial morphogenesis. *Curr Biol* 18:507-513.
9. O'Brien LE, Zegers MM, Mostov KE (2002) Building epithelial architecture: insights from three-dimensional culture models. *Nat Rev Mol Cell Biol* 3:531-537.
10. Park S, Ropella GE, Kim SH, Roberts MS, Hunt CA (2009) Computational strategies unravel and trace how liver disease changes hepatic drug disposition. *J Pharmacol Exp Therap* 328:294-305.
11. Robertson SH, Smith CK, Langhans AL, McLinden SE, Oberhardt MA, Jakab KR, Dzamba B, DeSimone DW, Papin JA, Peirce SM (2007) Multiscale computational analysis of *Xenopus laevis* morphogenesis reveals key insights of systems-level behavior. *BMC Syst Biol* 1:46.
12. Sausedo RA, Smith JL, Schoenwolf GC (1997) Role of nonrandomly oriented cell division in shaping and bending of the neural plate. *J Comp Neurol* 381:473-488.
13. Théry M, Racine V, Pépin A, Piel M, Chen Y, Sibarita JB, Bornens M (2005) The extracellular matrix guides the orientation of the cell division axis. *Nat Cell Biol* 7:947-953.
14. Théry M, Jiménez-Dalmaroni A, Racine V, Bornens M, Jülicher F (2007) Experimental and theoretical study of mitotic spindle orientation. *Nature* 447:493-496.
15. Thorne BC, Bailey AM, Peirce SM (2007) Combining experiments with multi-cell agent-based modeling to study biological tissue patterning. *Brief Bioinform* 8:245-257.
16. Wang Z, Zhang L, Sagotsky J, Deisboeck TS (2007) Simulating non-small cell lung cancer with a multiscale agent-based model. *Theor Biol Med Model* 4:50.
17. Yu W, Datta A, Leroy P, O'Brien LE, Mak G, Jou TS, Matlin KS, Mostov KE, Zegers MM (2005) Beta1-integrin orients epithelial polarity via Rac1 and laminin. *Mol Biol Cell* 16:433-445.
18. Zeigler BP, Kim TG, Praehofer H (2000) Theory of modeling and simulation: integrating discrete event and continuous complex dynamic systems. San Diego: Academic Press.

## Figures

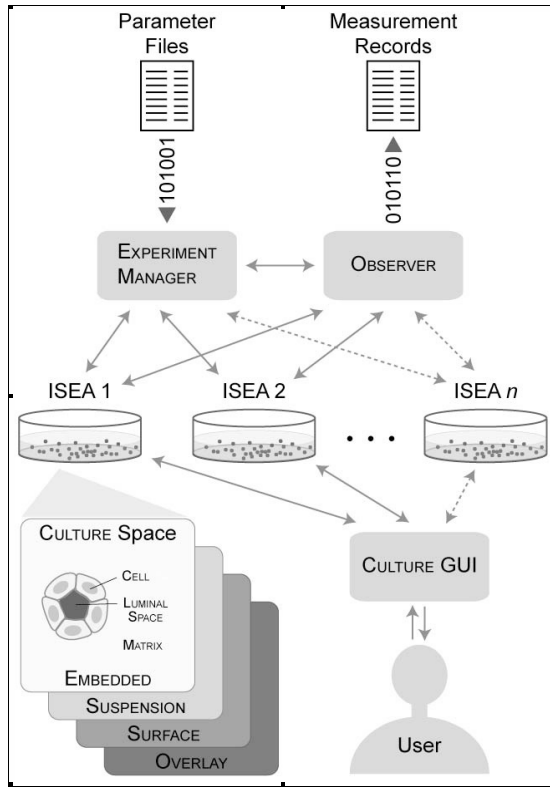


**Figure 3.1. ISEA components and system architecture**

The in silico system consists of a CULTURE and framework components. MDCK cell cultures and ISEAs are both composite systems. A CULTURE represents one *in vitro* cell culture. It is a composite of three object types: CELLS, MATRIX, and FREE SPACE. A hexagonal grid provides the space (CULTURE space) within which components interact. CELLS are quasi-autonomous agents whose actions are driven by their internal logic and a set of axiomatic operating principles. MATRIX maps to extracellular matrix, and FREE SPACE maps to aqueous material (e.g., cyst lumen) devoid of cells and matrix. Both are passive objects. ISEA1 (Grant et al., 2006) validated for basic, target attributes of four different cell culture types: embedded, suspension, surface, and overlay. ISEA1 was revised to ISEA2, which validated for an expanded set of target attributes. The framework provides components and methods to enable experimentation and analysis. EXPERIMENT MANAGER is the experiment control agent. It prepares parameter files, manages experiments, and processes data. OBSERVER is a module that automatically conducts and records measurements on CULTURE. CULTURE GUI provides a graphical interface to visualize and interactively probe CULTURE during execution.

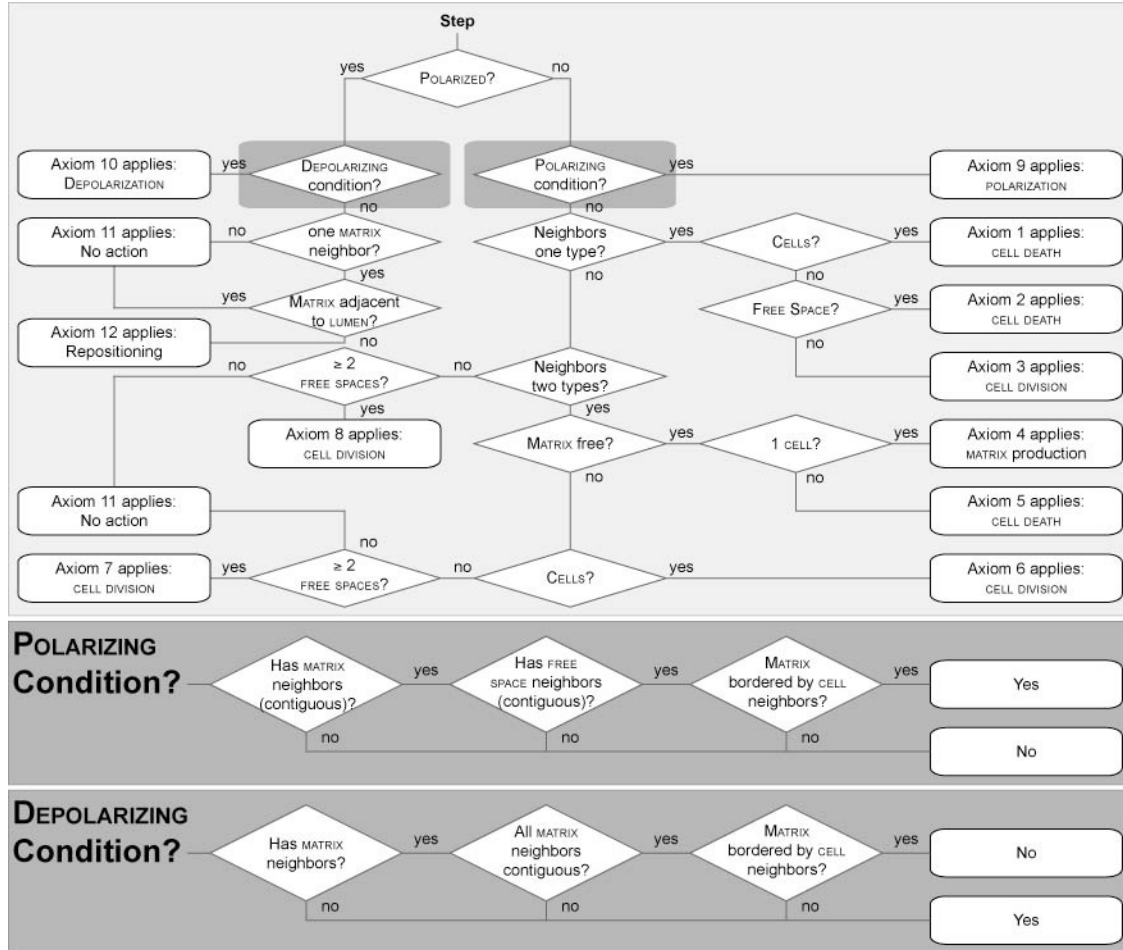


**Figure 3.2. ISEA2 CELL decision logic and axiomatic operating principles**

Simulation time advances by simulation cycles. During a simulation cycle, every CULTURE component is given an opportunity to update. Every CELL in a pseudo-random order decides what action to take based on its internal state (Polarized or Unpolarized) and the composition of its adjacent neighborhood. Actions available to Unpolarized CELL actions are: DIE, create a new CELL, produce MATRIX, POLARIZE, and do nothing. Polarized CELLS have three options: DEPOLARIZE, reposition, or do nothing. At every decision point, the CELL uses the diagrammed logic to select and execute just one action. I iteratively refined ISEA1 to ISEA2. It consistently produced convex, cystic structures in addition to achieving the original set of targeted attributes.

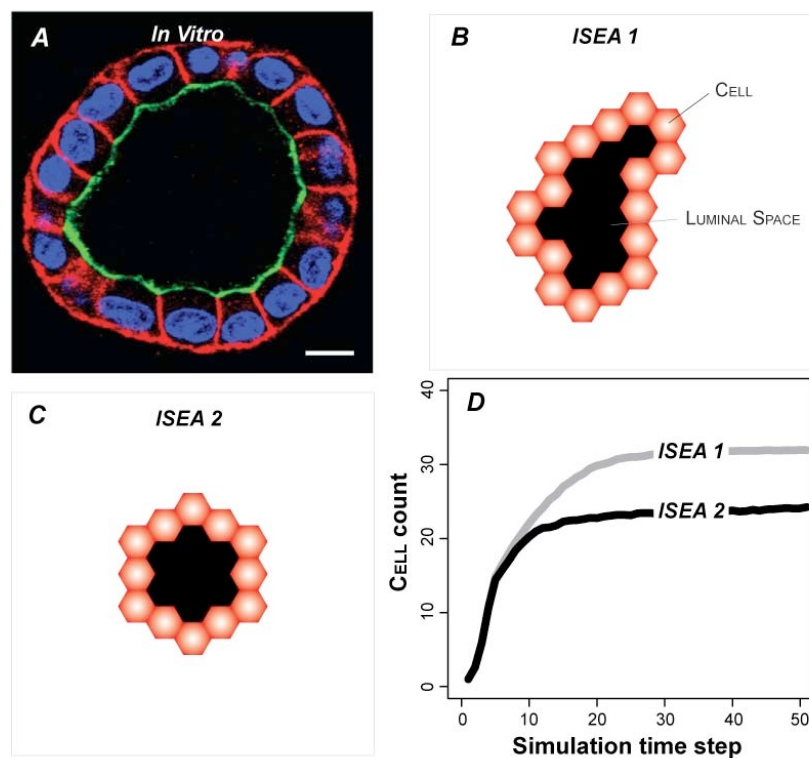


**Figure 3.3. Cyst growth in simulated and in vitro MDCK cell culture**

(A) MDCK cells grown in 3D matrix form lumen-enclosing cystic organoids surrounded by a layer of polarized cells. Cells composing the cysts maintain three surface types: apical (green), basal and lateral (red). Note the roundish contour typical of MDCK cysts. For growth and staining details, see (Yu et al., 2005). Bar: 10  $\mu\text{m}$ . (B) ISEA1 CELLS in EMBEDDED condition produced stable, cystic structures enclosing LUMINAL SPACE; all CELLS were POLARIZED (red). Many CYSTS like the one shown, had irregular, non-convex shapes unlike their in vitro counterpart. (C) ISEA2 CELLS under the same condition also developed stable CYSTS; almost all stabilized CYSTS had convex shapes. Note that a hexagonal CYST within the hexagonally discretized space maps to a roundish cross-section through a MDCK cyst in vitro. (D) ISEA2 CELLS formed CYSTS that tended to be smaller than those of ISEA1 (average 27 vs 31 CELLS per CYST). The CELL count represents mean values after 50 simulation cycles of 100 Monte Carlo runs.

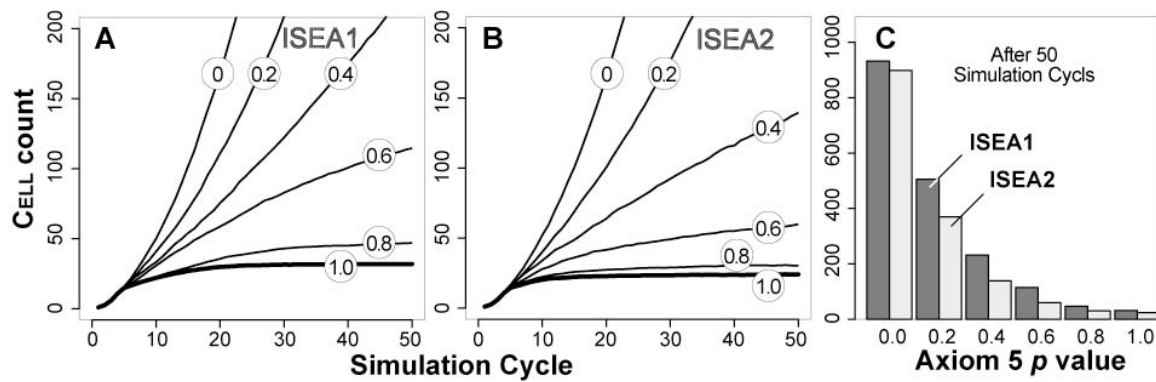


**Figure 3.4. Dysregulation of Axiom 5 (ANOIKIS) and its effect on ISEA growth and morphology**

Axiom 5 dictates CELL DEATH when the decision-making CELL has in its neighborhood at least two CELLS and LUMINAL SPACE but no MATRIX. CELLS followed Axiom 5 with a parameter-controlled probability,  $p$ . Otherwise, the Axiom 5 precondition produced no CELL DEATH. Evasion of Axiom 5 changed ISEA1 and ISEA2 growth and structural characteristics in EMBEDDED CULTURES. (A–B) CELL counts at six levels of dysregulation are shown. Values are means of 100 Monte Carlo runs. CELL count increased monotonically with the severity of dysregulation. For ISEA2, the effects were less dramatic for larger  $p$ . (C) Dysregulation caused a nonlinear increase in both ISEA1 and ISEA2 CELL count measured after 50 simulation cycles.

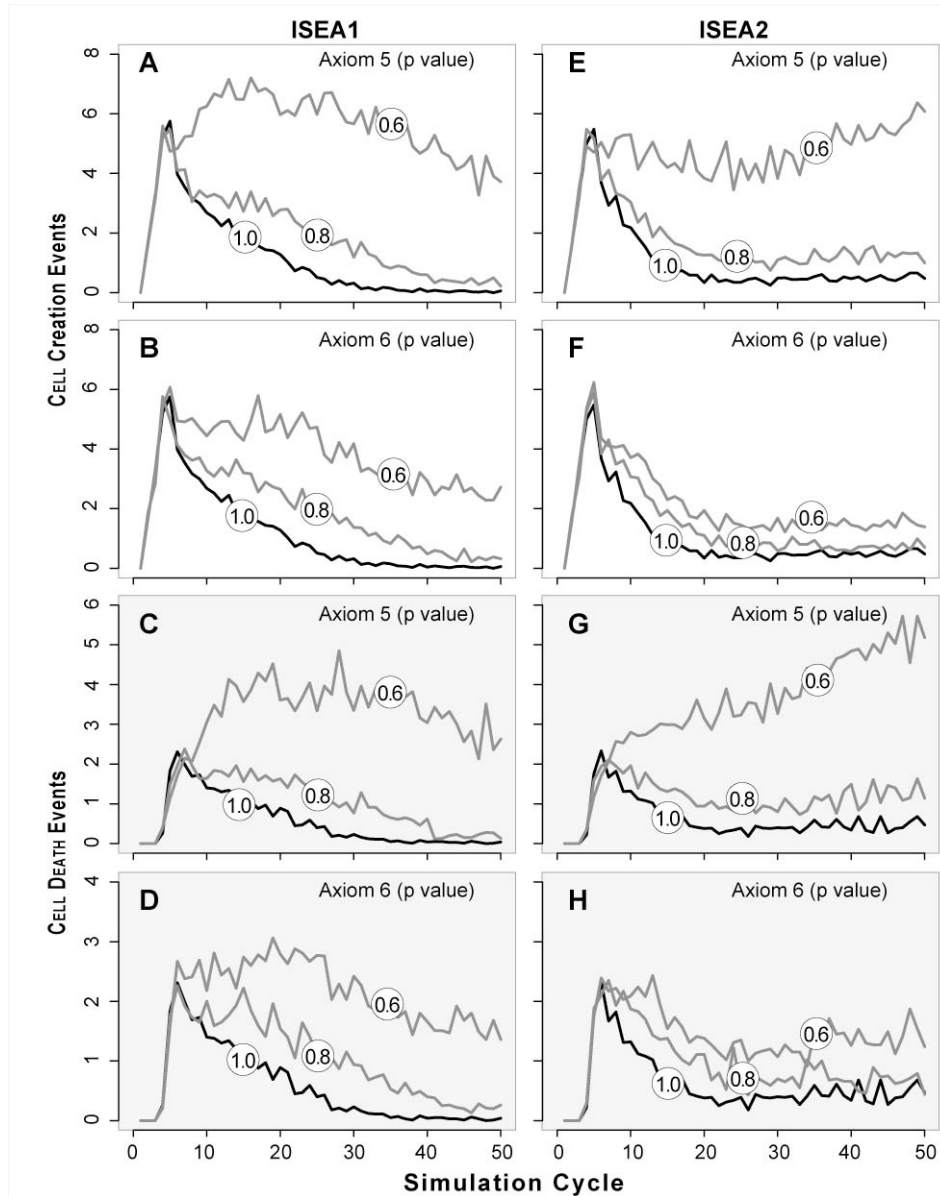


**Figure 3.5. CELL DEATH and creation events by ISEA1 and ISEA2 with and without dysregulation (two levels) of Axioms 5 and 6**

Values in circles are axiom  $p$  values. Left panels (A–D): ISEA1 events. Right panels (E–H): ISEA2 events. Top four panels: CELL creation events. Bottom four panels: CELL DEATH events. Event values are occurrences per simulation averaged over 100 Monte Carlo runs.

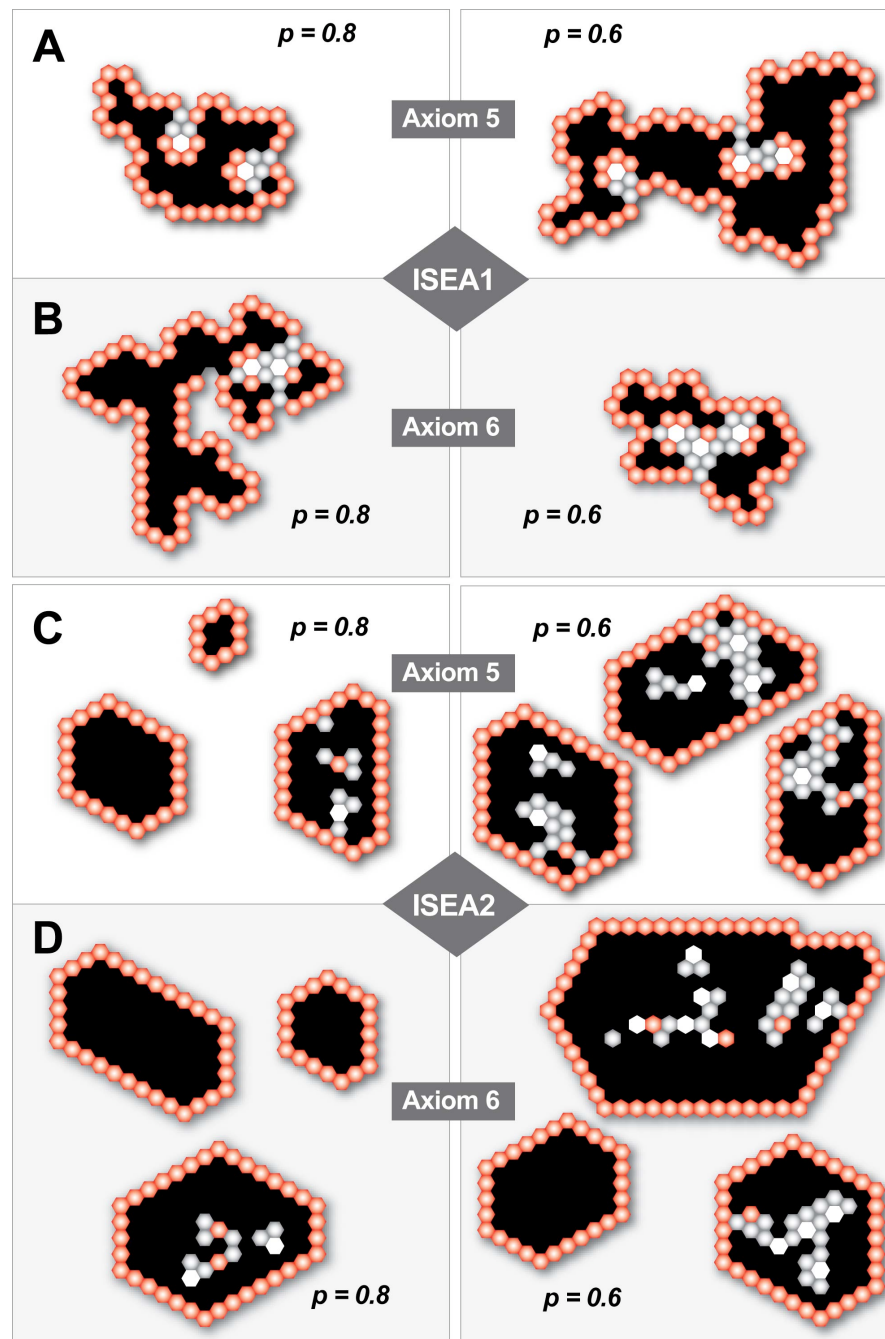


**Figure 3.6. Typical structures formed by ISEA1 and ISEA2 when Axiom 5 or 6 was dysregulated to five different degrees**

Shown are images of structures formed after 50 simulation cycles for  $p = 0.8$  and  $0.6$ . Note that a regular hexagon in 2D hexagonal space maps to a circle in 2D continuous space. Objects:

POLARIZED CELL (red), UNPOLARIZED CELL (gray), MATRIX (white), and LUMINAL SPACE (black).

(A–B) Shown are examples of structures formed when ISEA1 was dysregulated. (C–D) Shown are examples of structures formed when ISEA2 was dysregulated.

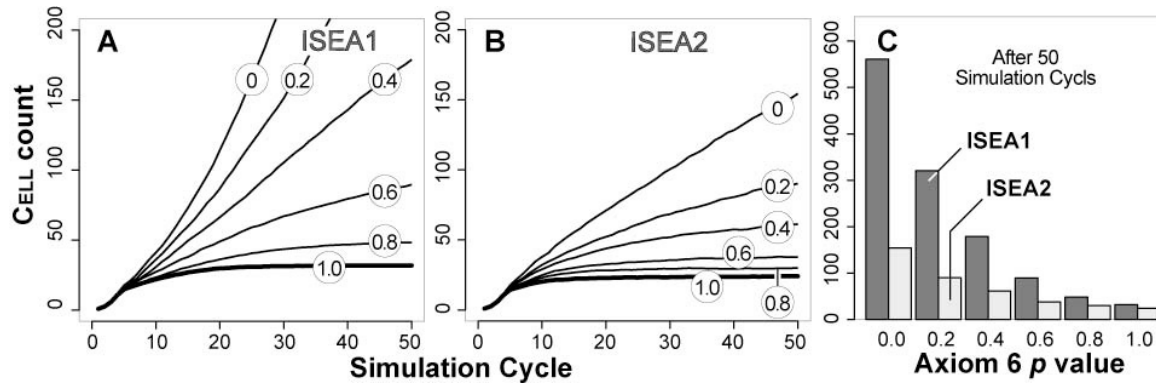


**Figure 3.7. Dysregulation of Axiom 6 and its effect on ISEA CULTURE growth**

Axiom 6 dictates oriented placement of a newly created CELL. It is placed at an adjacent MATRIX position that maximizes its number of CELL neighbors. CELLS followed Axiom 6 with a parameter-controlled probability,  $p$ . Otherwise, the CELL copy replaced a randomly selected MATRIX neighbor without regard for CELL neighbor number. Doing so changed ISEA growth and structural characteristics. (A–B) CELL count increased monotonically with the severity of dysregulation. Compared to ISEA1 growth (A), ISEA2 growth was affected less for every dysregulation level. (C) CELL count after 50 simulation cycles showed marked differences between ISEA1 and ISEA2 that increased with the severity of dysregulation.

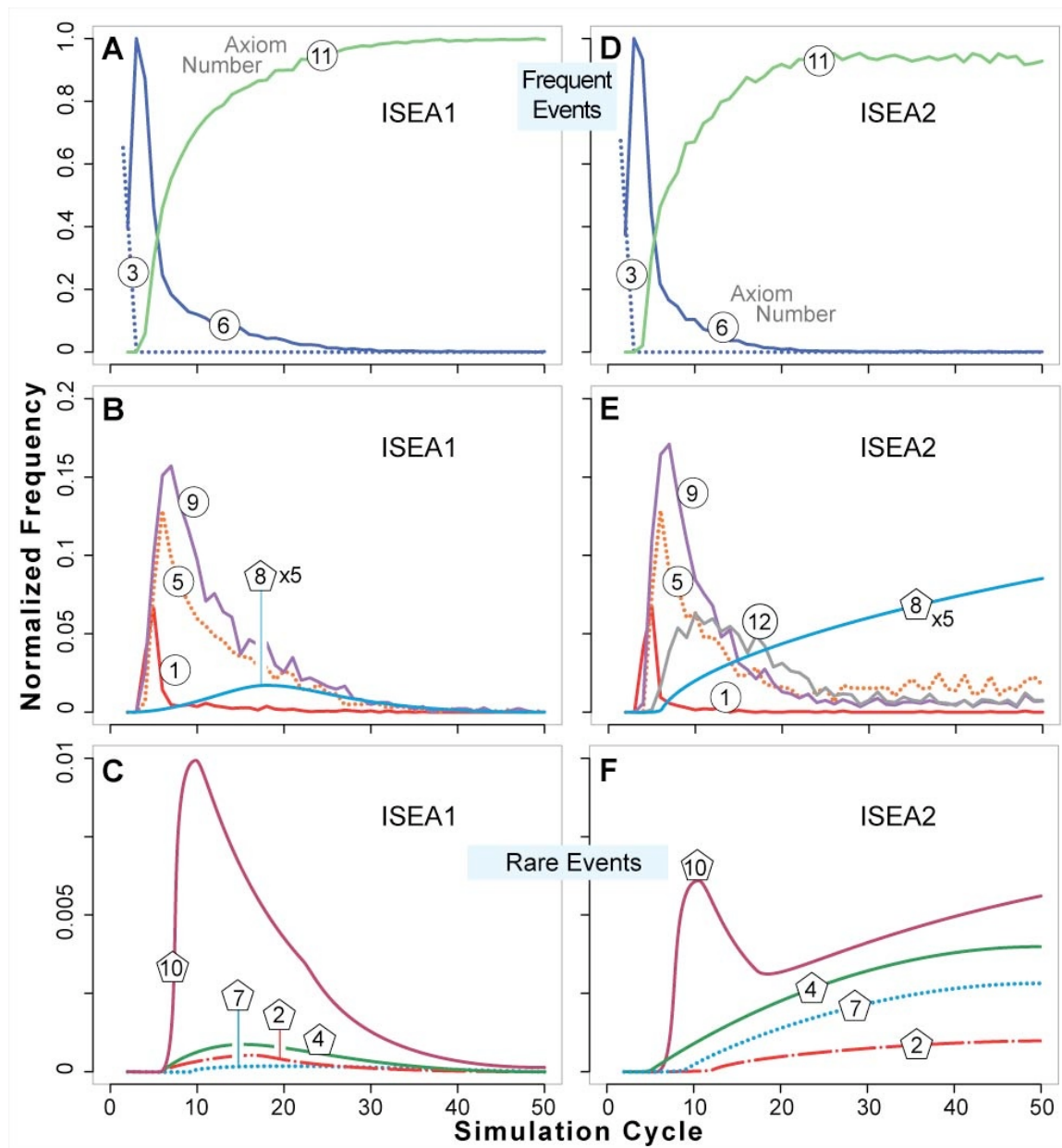


**Figure 3.8. Dynamic phenotype: axiom usage by ISEA1 and ISEA2**

Normalized axiom use frequencies are plotted versus simulation cycle. Left panels (A–C): ISEA1 use frequencies. Right panels (D–F): ISEA2 use frequencies. Top: axioms used most frequently. Middle: moderate use events. Bottom: Rare axiom use events. Axiom numbers in circles: the curves are normalized use frequencies averaged over 100 Monte Carlo runs. Axiom numbers in pentagons: the variance in average use frequency for the rarely used axioms was large; for clarity, trend lines are shown. In B and E, trend lines for Axiom 8 usage are magnified by a factor of 5. Raw data are provided in Supplemental Material. As simulations progressed and CYSTS matured, Axiom 11 (do nothing) was executed most frequently.

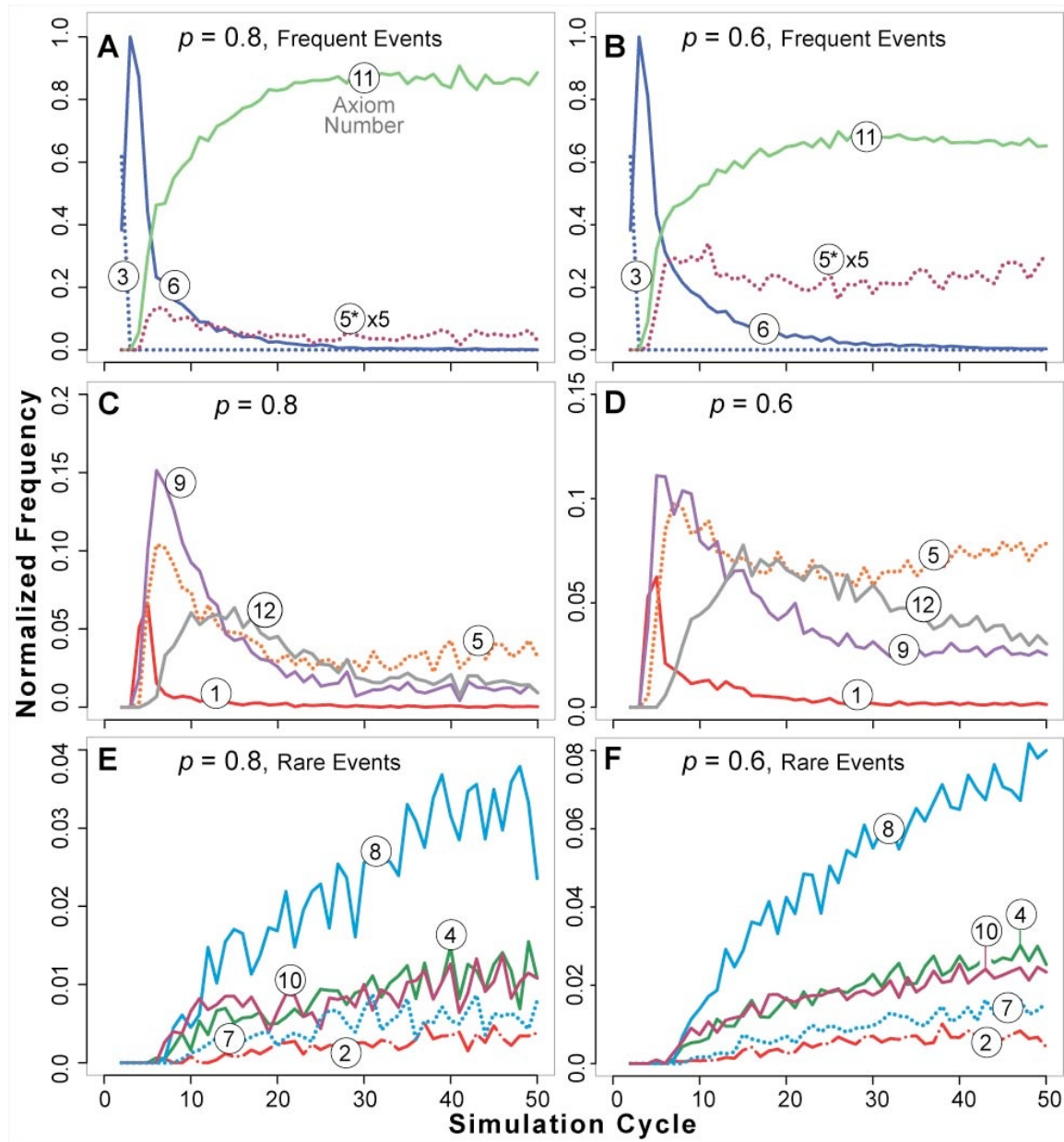


**Figure 3.9. Axiom usage by ISEA2 during partial Axiom 5 dysregulation**

Normalized axiom use frequencies are plotted versus simulation cycle as in Fig. 3.8. Axiom numbers in circles are shown for each curve. \*: dysregulated action. Left panels (A–C):  $p = 0.8$ . Right panels (D–F):  $p = 0.6$ . Top: axioms used most frequently. Middle: moderate use events. Bottom: Rare axiom use events. The curves are normalized use frequencies averaged over 100 Monte Carlo runs. In A and B, Axiom 5\* usage frequencies are magnified by a factor of 5.

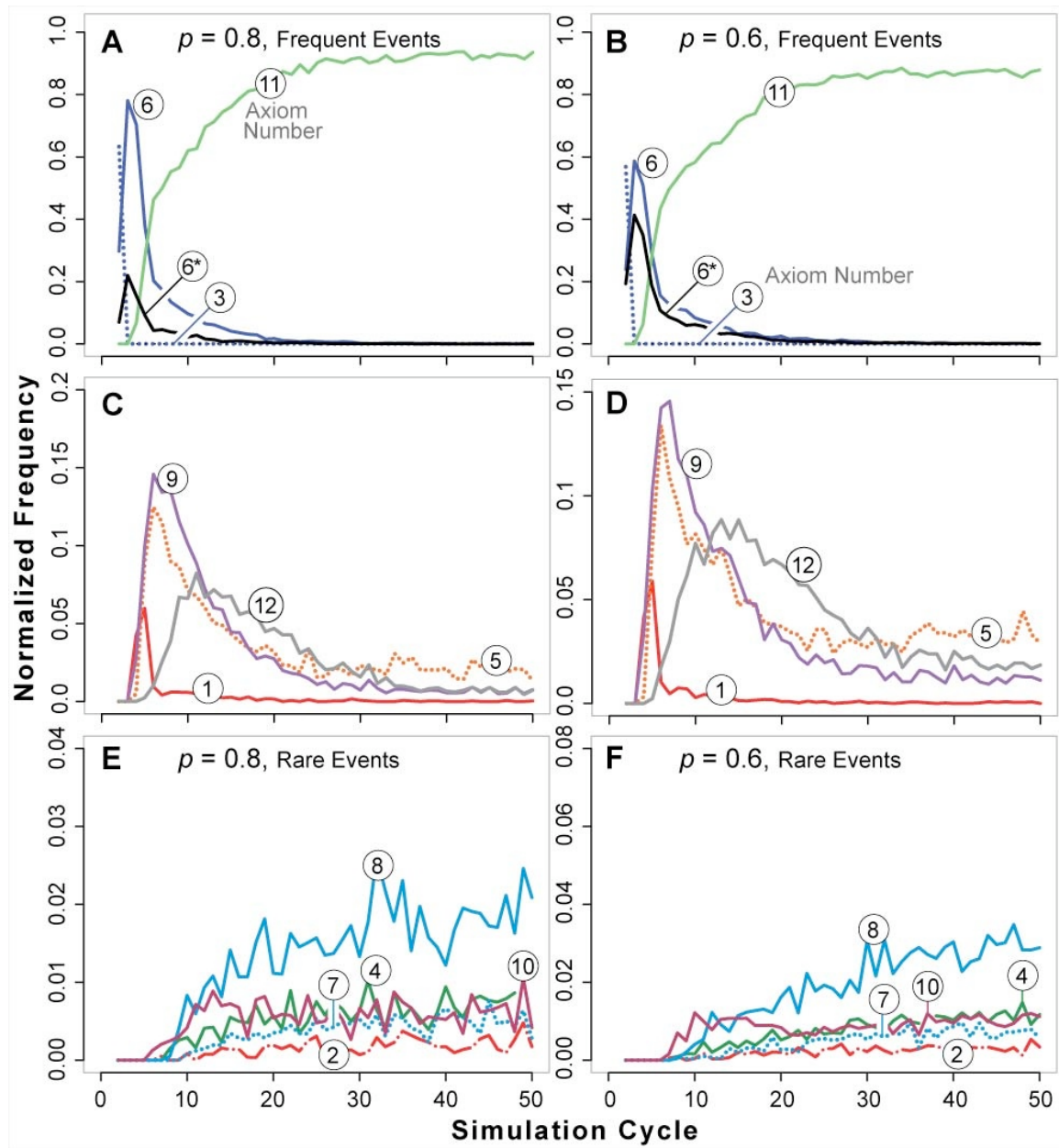


**Figure 3.10. Axiom usage by ISEA2 during partial Axiom 6 dysregulation**

Normalized axiom use frequencies are plotted versus simulation cycle as in Figs. 3.8 and 3.9. Axiom numbers in circles are shown for each curve. \*: dysregulated action. Left panels (A–C):  $p = 0.8$ . Right panels (D–F):  $p = 0.6$ . Top: axioms used most frequently. Middle: moderate use events. Bottom: Rare axiom use events. The curves are normalized use frequencies averaged over 100 Monte Carlo runs.